Limnol. Oceanogr., 54(6), 2009, 2081–2088

Climate variation, carbon flux, and bioturbation in the abyssal North Pacific

Michael F. Vardaro,[a,*] Henry A. Ruhl,[b] and Kenneth L. Smith, Jr.[a]

[a] Monterey Bay Aquarium Research Institute, Moss Landing, California
[b] National Oceanography Centre, Southampton, Waterfront Campus, Southampton, UK

Abstract

We hypothesized that seasonal and interannual climate-mediated changes in particulate organic carbon (POC) flux would affect bioturbation and ultimately the sequestration of organic carbon in the deep sea. An 18-yr time-series photographic record from 4100-m depth in the northeast Pacific Ocean showed increased abundance of *Echinocrepis rostrata*, a common epibenthic echinoid and bioturbator, since the late 1990s. Abundance, size, and speed data were used to estimate bioturbation potential to track long-term changes in the volume of sediment disturbed by *E. rostrata*. There was no secular increase in *E. rostrata* bioturbation over 18 yr despite increased population size, although periodic variations in bioturbation were significantly correlated with POC flux. Expected changes in POC flux and bioturbation rates due to climate variation could lead to altered rates of carbon sequestration in deep-sea sediments, affecting the global carbon cycle.

Fluctuations in climate influence deep-sea benthic community structure and activity through the marine carbon cycle. Climate variation affects levels of photosynthetic activity at the sea surface and subsequent particle export (Kahru and Mitchell 2002; Buesseler et al. 2007). Ocean warming is likely to increase stratification and decrease nutrient availability at the surface, leading to a shift toward smaller phytoplankton, greater recycling of nutrients in surface layers, and decreases in particulate organic carbon (POC) flux out of the euphotic zone (Bopp et al. 2005). Thus photosynthetic activity and primary production are related to the quantity and quality of POC flux that reaches the seafloor and ultimately influences the benthic community (Smith et al. 1994; Ruhl and Smith 2004; Ruhl 2007).

Although flux attenuation rates are variable, the majority of the organic carbon produced in the surface layers of the ocean is either recycled in the upper ocean (Martin et al. 1987; Buesseler et al. 2007) or gradually consumed and remineralized as it falls through the water column (Lee et al. 1998; Stemmann et al. 2004). Organic carbon that reaches the seafloor provides food for benthic fauna and some portion becomes sequestered through burial either before or after being ingested (Reimers et al. 1992; Levin et al. 1999; Smallwood et al. 1999). The fate of POC that reaches the seafloor is heavily influenced by the actions of benthic megafauna that feed on or bury the surface-derived phytodetritus (Aller 1982; Smallwood et al. 1999). Here we show that climate variation and bioturbation at a site in the deep North Pacific (Sta. M; 34°50′N, 123°00′W; 4100 m depth) are positively correlated, and that increased POC flux leads to increased rates of bioturbation, an important carbon sequestration dynamic.

Echinocrepis rostrata, a deep-sea epibenthic, irregular echinoid, is common at Sta. M and leaves distinctive trails in the sediment that allow quantification of the volume disturbed by their movements. Abundance, body size, and speed of *E. rostrata* from the photographic record were used to create an equation describing *E. rostrata* bioturbation potential, similar to that generated for shallow-water environments (Solan et al. 2004; Lohrer et al. 2005). Unlike prior research, which used indices of bioturbation to compare the relative contributions of multiple epibenthic and infaunal populations with total sediment mixing rates in shallow water (Solan et al. 2004), our study focused on the primary species, *E. rostrata*, as a proxy for sediment disturbance in a deep-sea environment with few large epibenthic bioturbators. The traits used in our calculation of the sediment volume disturbed by *E. rostrata* bioturbation (B_i, mm^3 m^{-2} d^{-1}) were abundance (A_i, individuals m^{-2}), size (S_i, mm), movement speed (V_i, mm d^{-1}), and depth of sediment disturbance (D_i, mm):

$$B_i = A_i \times S_i \times V_i \times D_i \quad (1)$$

Full descriptions of each trait and the details of their derivation from camera sled (CS) and time-lapse camera (TLC) data sets are provided in the Methods and Results section.

Methods

TLC—The TLC system was first deployed at Sta. M in 1989 (Smith et al. 1993) and continued through September 2007, collecting 27 time-lapse image data sets of approximately 4 months each. The camera took one oblique photograph of the seafloor every hour (Fig. 1a) and was serviced three times a year. The TLC consisted of a Benthos 377 camera mounted on a titanium frame at an angle of 31° from horizontal with the lens ~2 m above the seafloor. The camera was equipped with a 28-mm Nikonos lens, providing angular coverage of 50° in the horizontal and 35° in the vertical plane, and held 400 feet of 35-mm color-negative film (Fuji, type 8514, 500 ASA). Up to 3500 images could be collected in 4–6 months. Two 400-W s strobes, one mounted on either side of the camera housing,

* Corresponding author: mvardaro@mbari.org

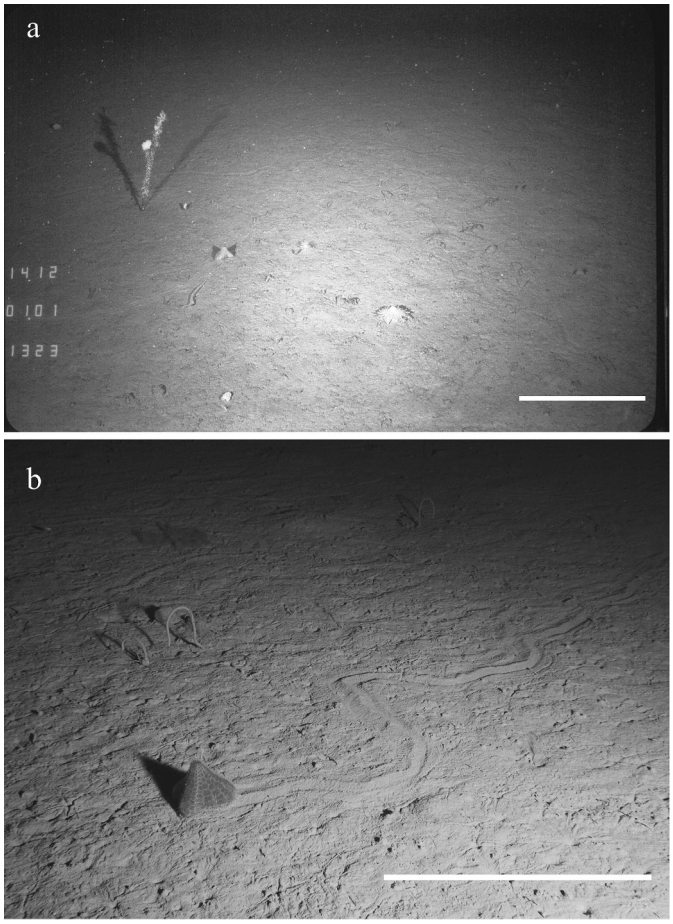

Fig. 1. Examples of images from the (a) autonomous time-lapse camera record and the (b) towed camera sled footage taken at Sta. M, with an *Echinocrepis rostrata* visible in the center of the field of view in each shot. The characteristic trail left in the sediment by *E. rostrata* movement is markedly evident in the camera sled image. Scale bar is 0.5 m in both images.

illuminated approximately 20 m^2 of the seafloor beginning at a distance of 1.8 m from the camera frame and extending approximately 6.5 m from the base of the camera frame (Smith et al. 1993 for a more complete description of the TLC).

CS—Fifty-two seasonal photographic line transects were also taken using a towed CS between October 1989 and October 2004. The CS data was used to evaluate the abundance and average body size over time because of the greater spatial coverage of the line transects (~125,797 m^2) compared with the TLC area (~560 m^2). Although abundance can be calculated from stationary measurements or "point transects," the mobility of *E. rostrata*, the total number of individuals seen in the TLC records (n_{TLC} = 202), and the low number of individuals visible in the camera field of view at a particular point in time made it less appropriate to rely on TLC-based abundance values. Because of logistical restraints, the frequency of these transects was variable, but they were typically conducted seasonally. Line-transect photography was conducted using a Benthos 372 35-mm film camera and Benthos 382 strobe mounted on a towed benthic CS, at a height of 82 cm and 22.5° below horizontal. The camera took one photograph every 5 s as the sled moved along the bottom at ~2.8 km h^{-1}. The overlapping images created a continuous image mosaic of the seafloor. A semiballoon otter trawl net towed behind the CS collected specimens from the line-transect area. Specimens recovered from the trawl net were then identified and used to facilitate identification of the species observed in the line-transect photographs. The trawl net had a 6.1-m opening and a 3.8-cm stretch mesh net with a 1.3-cm mesh cod-end liner. The resulting photographic record monitored the benthic community over 18 yr. The CS tows provided instantaneous line-transect measurements of epibenthic megafauna abundance and size, whereas the TLC system monitored a single area of the seafloor for 4-month intervals with a detailed view of temporal changes in activity and bioturbation (Fig. 2a,b). Animal specimens were collected by remotely operated vehicle (ROV) and submersible during research cruises in 2006 and 2007.

Photographic analysis—The oblique photographs taken by the TLC were analyzed using a perspective-grid method (Wakefield and Genin 1987). Each image was projected onto a flat surface and digitized with a Science Accessories Corp.® electronic digitizer interfaced with a computer. The CS photographs were evaluated using a Canadian grid system (Wakefield and Genin 1987) as well as the computer program DISTANCE (Laake et al. 1994). Using the digitized location of each individual along each transect, DISTANCE estimated the visibility of an object at a distance perpendicular to the centerline of the transect. The DISTANCE program then provided a probability density function and effective strip width (ESW) for each species. The transect length was calculated using the sum of nonoverlapping distances between frames along the axis of the transect. Overlap was estimated by measuring the relative positions of objects visible in sequential frames. The ESW was multiplied by the transect length to provide an estimation of abundance.

Sizes of *E. rostrata* for the bioturbation calculations were taken from the CS data rather than the TLC data again because of the much larger sample size. Size drawn from the CS photographs was of body length rather than the anterior width. Since anterior width corresponds to the width of the trails of disturbed sediment left by *E. rostrata* movement, we converted the length to width measurements using a ratio (length : anterior width) derived from measurements taken of 98 *E. rostrata* specimens collected by ROV and submersible.

Climate and upwelling indices—Four indices were examined as part of this study: the Northern Oscillation Index (NOI, Schwing et al. 2002), Southern Oscillation Index (SOI, Trenberth and Shea 1987), the Multivariate El Niño–Southern Oscillation Index (MEI, Wolter and Timlin 1998), and the Bakun Upwelling Index (BUI, Bakun 1973). The NOI is based on the difference in sea level air pressure anomalies between a location in the NE Pacific and a region near Darwin, Australia. The SOI is analogous

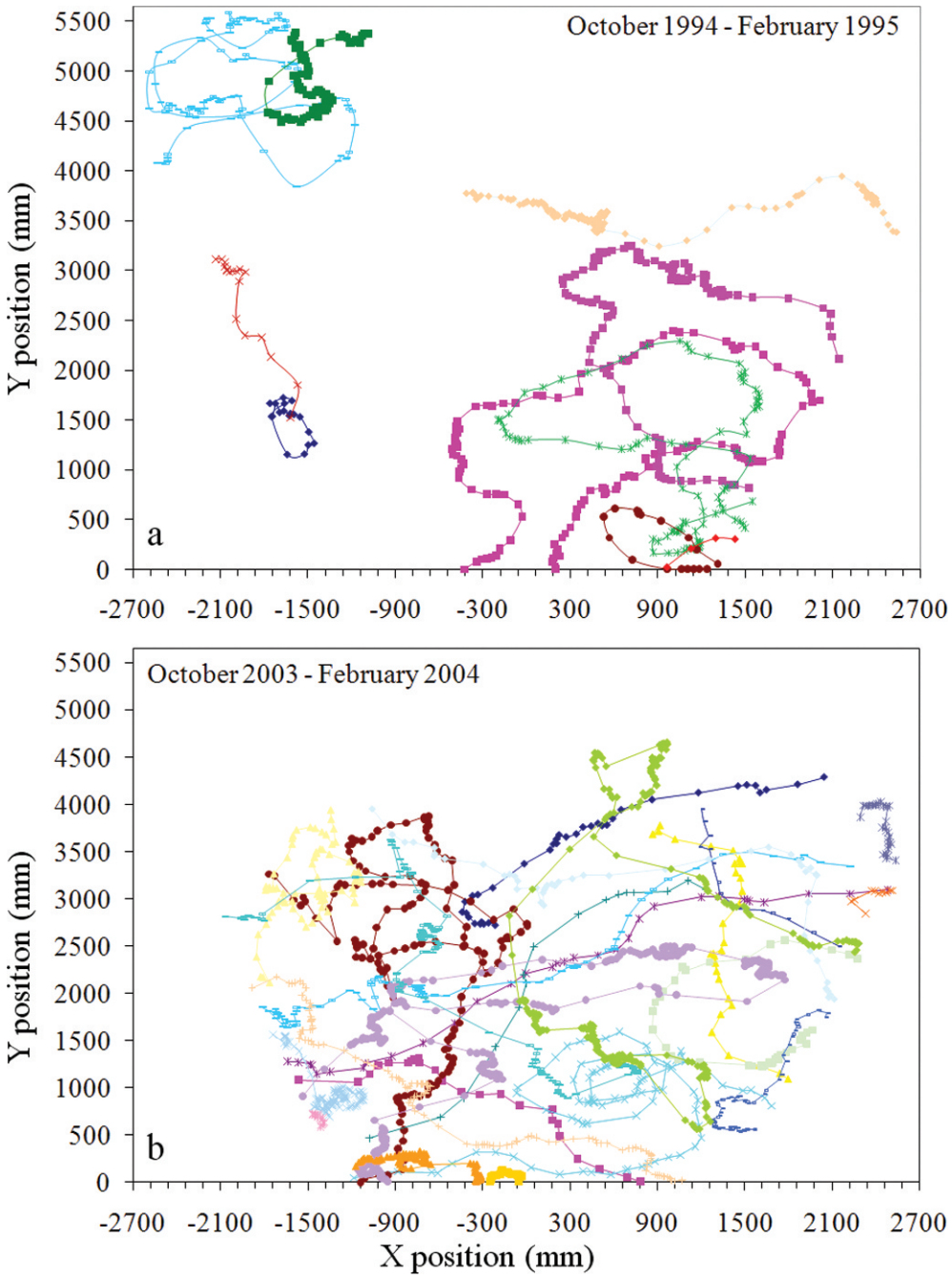

Fig. 2. *Echinocrepis rostrata* movement patterns digitized from 4-month (October to February) autonomous time-lapse camera deployment periods at Sta. M (a) before and (b) after the 1998 El Niño–La Niña cycle. These time periods illustrate the observed increase in *E. rostrata* abundance between 1998 and 2005. Each colored line indicates an individual *E. rostrata* trail through the field of view of the camera; units are in millimeters from the base of the field of view and the intervals between plotted points are hours.

to the NOI, but is based on two South Pacific locations. The NOI is correlated more closely with ecological variables in the NE Pacific, although both the NOI and SOI are highly correlated (Schwing et al. 2002). The MEI is an anomaly index that incorporates parameters such as sea surface temperature, clouds, and wind (Wolter and Timlin 1998). Correlations with the MEI have the opposite sign of correlations with the NOI and SOI. The BUI is measure of the volume of water that upwells along the coast. It uses geostrophic wind fields to identify the amount of offshore transport of coastal surface waters.

All time-lagged correlations used the nonparametric Spearman rank correlation with monthly data and 1-month lag intervals. Pearson (parametric) correlations have several assumptions that are violated by the biological data in this study, including normality and homoscedasticity.

Nonparametric tests were used here since they do not make assumptions about the distribution of the data. Numerical analyses were done using Excel (Microsoft®) and Statistica (StatSoft®). Conclusions regarding links with climate or food supply were based, in part, on whether the correlations met the basic criteria of sensible sign and temporal relationship specified in Ruhl and Smith (2004).

POC flux—POC flux to the seafloor was measured using two Teflon©-coated McLane PARFLUX©-style sediment traps with 0.25-m^2 openings moored at 50 m above bottom (mab; 4050 m water depth) and 600 mab (3500 m water depth). Ten-day samples were taken at 50 and 600 mab. Details of sediment trap data collection and analysis can be found in Baldwin et al. (1998). Temporal gaps in measured POC flux measurements over the time series necessitated the creation of a composite estimate of POC flux. This POC flux composite incorporates POC flux data from 50 mab, then uses available data from the 600-mab sediment trap to fill in gaps where possible, and finally an estimation of POC flux to 50 mab on the basis of multiple regression analysis of empirical data. A detailed description of how the POC flux composite was generated can be found in Smith et al. (2006) and Ruhl (2008). The composite of both measured values and model-estimated values presented a nearly continuous POC flux time series to cross-correlate with climatic indices, bioturbation rate, and the parameters used to calculate the bioturbation rate (abundance, size, and speed).

Results

We derived the abundance of *E. rostrata* principally from the CS line transects, which provided a more robust measurement of abundance changes over time. An order-of-magnitude increase in *E. rostrata* abundance (Fig. 3a) occurred between 1998 (0.01–0.02 individuals m^{-2}) and 2005 (0.80–0.12 individuals m^{-2}) and was recorded from the CS transects (Ruhl 2007). A similar trend was seen in the number of *E. rostrata* drawn from the TLC data. The average yearly number of *E. rostrata* seen in the field of view of the TLC before 2000 was 0.4 individuals m^{-2} (Fig. 2a), which doubled to 0.8 individuals m^{-2} after 2000 (Fig. 2b).

The increase in abundance coincided with a decrease in the mean width of the individuals observed per month in both the CS (Ruhl 2007) and TLC photographic records. Monthly mean widths of *E. rostrata* observed by the CS decreased from 62 mm (±9 mm) before 2000 to 43 mm (±13 mm) after 2000 (Fig. 3a); however, the decrease in size seen in the TLC data fell within the error range. The disparity between the significance of the *E. rostrata* size changes observed in the CS data and the nonsignificant change seen in the TLC data was most likely due to the differences in spatial coverage and sample size. The CS camera, at ~1 m above the seafloor, facilitated measurements of smaller *E. rostrata* individuals and the greater spatial coverage enabled the CS to photograph a larger number of individuals (n_{CS} = 2782) than the TLC (n_{TLC} = 202).

Mean speed of *E. rostrata* individuals observed by the TLC (1.68 ± 0.85 m d^{-1}) did not exhibit a significant monotonic trend (p = 0.55) over the entire time series, from 1989 to 2007, and a Mann–Whitney test showed no significant difference (p = 0.31) between mean movement speeds from 1989 to 1998 and those from 2000 to 2006 (Fig. 3a). However, a seasonal pattern in *E. rostrata* movement speed did emerge. Speed correlated significantly (r_s = 0.29; p = 0.01) with sea surface temperature, which had a primarily seasonal variation during the study period, in a nonparametric Spearman correlation. There was also a significant positive correlation (r_s = 0.36; $p = 1.85 \times 10^{-6}$) between the size of *E. rostrata* individuals and their speed.

The mode of *E. rostrata* bioturbation, ''plowing'' through the top layer of the sediment, remained consistent in both TLC and CS photographic records. No *E. rostrata* were observed in the process of burrowing into the sediment; however, on a few occasions some individuals were coated with sufficient sediment to be nearly obscured. Although not able to be reliably measured from either TLC or CS photographs, furrow depth was determined by comparing the measured heights of collected *E. rostrata* individuals with the depth of the furrows they were observed creating in ROV and submersible video footage. The depth of the trails produced by the *E. rostrata* observed and collected during submersible and ROV dives at Sta. M ranged from 0- to 2-cm depth. Here we use an estimated mixing depth of 1 cm in the bioturbation equation.

The quantity of bioturbation values (n = 16) was a product of the occasional lack of temporal overlap between CS and TLC deployments. There was a total of 37 months with *E. rostrata* abundance and size data from the CS tows, but only 16 of those months also included TLC deployments with visible *E. rostrata* that allowed measurement of movement speed and estimation of the bioturbation rate.

The amount of sediment disturbance by *E. rostrata* calculated by using the above values was positively correlated (r_s = 0.65; p = 0.009) to POC flux to the seafloor, with periodic changes in bioturbation rate lagging variations in food supply by ~1 month (Table 1). However, there was no secular change in the *E. rostrata* bioturbation rate (p = 0.762) over the length of the time-series record (Fig. 3a). The lack of long-term nonperiodic change in *E. rostrata* bioturbation was not unexpected because of the relationship with POC flux. POC flux has also not undergone any secular change over the time period of the time series. The long-term trends seen in the variables used to calculate bioturbation show either no secular change (speed, trail depth) or a negative correlation (size vs. abundance; Fig. 3b).

POC flux has previously been correlated to upwelling indicators such as the BUI (Fig. 3d), with time lags between upwelling events and changes in the food supply to the deep sea of ~40 to 60 d at Sta. M (Baldwin et al. 1998). Climate indices expressive of El Niño–La Niña such as the NOI, the MEI (Fig. 3c), and the SOI have also been correlated with POC flux variations and shifts in benthic megafauna abundance (Ruhl and Smith 2004). Cross-correlations between NOI, SOI, and MEI climate indices and several holothuroid species abundances peaked with abundance lagging climate by 11 to 22 months (Ruhl and Smith 2004). We found that bioturbation by *E. rostrata* was also correlated with these indices at time lags varying from 3 to 4 months for the BUI, and 16–20 months for the NOI,

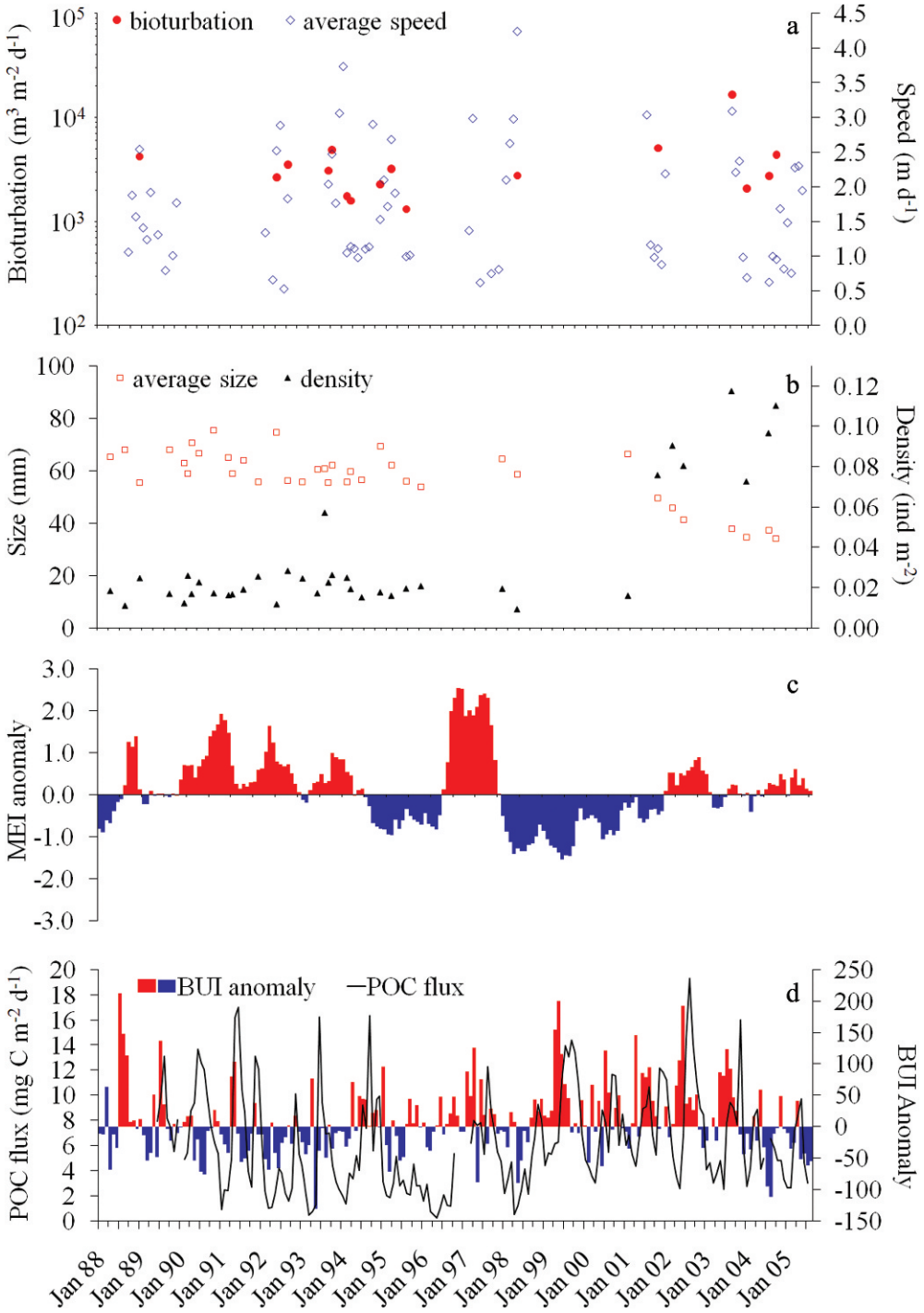

Fig. 3. (a) *Echinocrepis rostrata* bioturbation (circles) and speed (open diamonds), (b) the inverse relationship between *E. rostrata* size (open squares) and density (closed triangles) previously published in Ruhl (2007), (c) the MEI climate index anomaly, and (d) the POC flux composite (black line) and the BUI anomaly (red and blue bars), from 1989 to 2005.

SOI, and MEI (Table 1). The varying time-lags between changes in climate, temperature, upwelling, and bioturbation were not as clear-cut as anticipated, but can be attributed to the time necessary for climate variations to affect upwelling and POC flux and for the ensuing flux changes to be manifested in the seafloor community parameters. The parameters used to calculate the bioturbation rate (abundance, size, and speed) correlated with POC flux variations on differing timescales. *E. rostrata* abundance peaks lagged ~3 months behind POC flux changes, but there was no significant relationship between size and POC flux. Conversely, rates of speed shifted nearly instantaneously, with peaks lagging POC flux by ~0–1 month (Table 1). Speed of *E. rostrata* movement also

Table 1. Peaks in time-lagged Spearman rank cross-correlations (r) between climate indices and the factors used to calculate the index of bioturbation of *E. rostrata*. The correlations and associated time lags (in months) shown in the table are the peaks in cross-correlations (those with the highest r) and are not intended to represent fixed temporal lags. Bold text indicates significant ($p < 0.05$) correlations. n = number of monthly estimates for each correlation.

		POC flux			BUI			NOI			SOI			MEI		
Category	n	r	p	Time lag	r	p	Time lag	r	p	Time lag	r	p	Time lag	r	p	Time lag
Density	37	**0.39**	**0.020**	**3**	**0.46**	**0.004**	**4**	0.16	0.333	11	0.15	0.368	9	−0.18	0.283	13
Size	37	−0.12	0.473	3	−0.30	0.067	5	0.22	0.184	10	0.14	0.408	14	−0.23	0.162	20
Speed	71	**0.38**	**0.001**	**1**	**0.37**	**0.001**	**4**	0.007	0.949	7	0.08	0.501	11	−0.01	0.934	10
Bioturbation	16	**0.65**	**0.009**	**1**	**0.59**	**0.015**	**4**	0.39	0.137	16	**0.53**	**0.046**	**18**	**−0.51**	**0.041**	**20**
POC flux	206				**0.46**	**3.86×10^{-12}**	**2**	**0.47**	**1.86×10^{-12}**	**6**	**0.36**	**9.46×10^{-8}**	**10**	**−0.45**	**1.11×10^{-11}**	**9**

appeared to have seasonal peaks, coinciding with similar peaks in POC flux (Fig. 3a,d). The temporal lags between climate and bioturbation are the net outcome of changes in size, density, and speed.

The simplified sequence of events appears to unfold as follows: POC arrives on the seafloor, immediately increasing *E. rostrata* movement speed. Then, ~3–4 months later, abundance increases and average size declines (roughly simultaneously) with mixed effects on activity and bioturbation. The net result of increased POC flux on the above factors is manifested as an increase in *E. rostrata* bioturbation after ~1 month (Table 1).

Discussion

Epibenthic megafauna feeding and movement have proven to be major factors in incorporating detritus into the benthic food web. Detrital material that reaches the seafloor attracts epibenthic fauna that respond to these patches of resources (Levinton and Kelaher 2004; Ruhl and Smith 2004). These epibenthic megafauna then facilitate incorporation of the POC into the sediment where it is rapidly consumed by infauna (Smith et al. 1997; Levin et al. 1999) and bacteria (Smith et al. 1997). If the activity levels of epibenthic megafauna, such as the indicator species *E. rostrata*, are affected by climate-mediated changes in POC flux, the fate of carbon that reaches the seafloor will also be affected.

The time series used here is the most detailed available for mobile megafauna sediment disturbance in abyssal habitats. Data records of greater resolution or duration may yet reveal important seasonal or secular trends in bioturbation rates. For example, a paired t-test showed that there were significantly fewer occurrences ($p = 0.009$) of *E. rostrata* in TLC photographs during summer months than during winter months (Fig. 4). However, no seasonal pattern was found in the CS abundance data, which may indicate that the difference in the frequency of occurrence variation between TLC and CS abundances was primarily due to changes in movement speed or migration behavior rather than a localized change in population size. These behavioral changes, as well as size and abundance variation, would affect local bioturbation rates. Given the similar processes observed between Sta. M and other abyssal habitats, such as the Porcupine Abyssal Plain (Billett et al. 2001; Ruhl and Smith 2004) and the equatorial Pacific (Smith et al. 1997), broader effects on sediment mixing over regional to basin scales can be rationally extrapolated from the Sta. M data.

Shifting rates of bioturbation linked to climate could markedly affect sediment biogeochemistry. If global warming leads to increased stratification of ocean layers and decreased particle flux (Bopp et al. 2005), the results here suggest that rates of bioturbation would also decline. Decreasing rates of bioturbation would weaken sediment mixing, leading to reduced availability of surface-derived POC to deep-sea infauna and microbes (Reimers et al. 1992; Smallwood et al. 1999), resulting in reduced incorporation of surface-derived carbon into the infaunal food web (Aller 1982). Less sediment mixing by epibenthic megafauna could potentially strain infauna and microbial populations

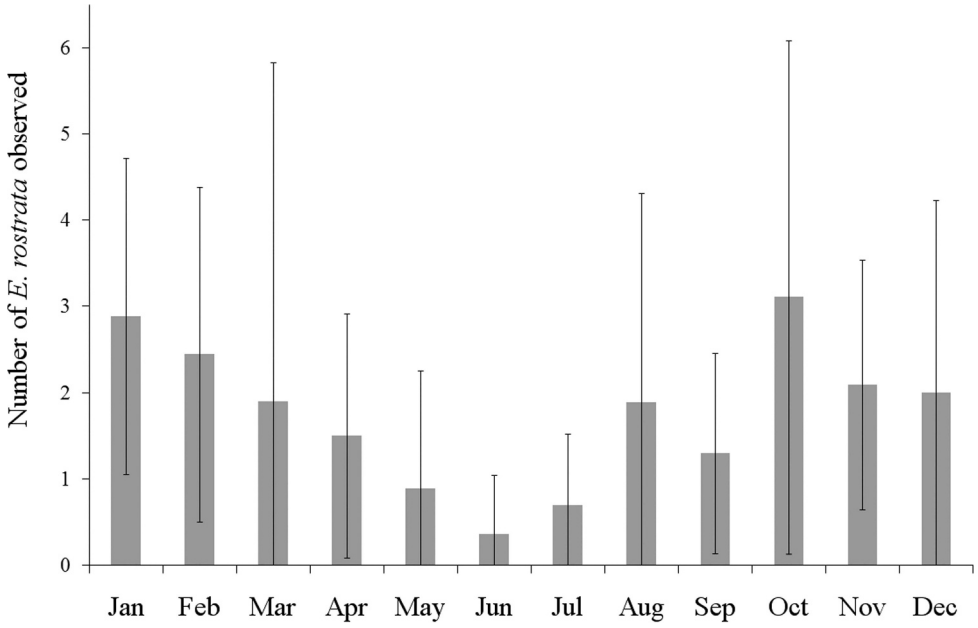

Fig. 4. A paired *t*-test showed a seasonal signal ($p = 0.009$) in the monthly average number of *E. rostrata* individuals observed over the 18-yr time-lapse camera record. The error bars indicate one standard deviation.

that depend on the transport of POC deposits from the sediment–water interface deeper into the sediment (Danovaro et al. 2008; Thistle et al. 2008). Restructuring of the benthic community and the rise of new dominant species might also follow such changes in sediment mixing.

Variation in sediment stratification and species composition due to changes in bioturbation rates (Guinasso and Schink 1975) can provide a means of tracking climatic shifts in the geologic record (Behl and Kennett 1996). Diversity oscillations and significant abundance changes in deep-sea benthic species have been linked to variation in climate both in the geologic record (Yasuhara et al. 2008) and in contemporary benthic surveys (Ruhl and Smith 2004; Ruhl 2008). Declines in sediment mixing and phytodetritus breakdown by benthic infauna and microbes combined with the decomposition of the food-deprived infaunal population could lead to reductions in dissolved oxygen in the sediment and a positive feedback loop that could even further reduce levels of bioturbation. Although even total anoxia does not preclude the breakdown of phytodetritus on the seafloor (Hulthe et al. 1998), the combined effect of reduced bioturbation and lower sediment oxygenation on the benthic community might fundamentally change the ability of the benthos to respond to and break down large pulses of phytodetritus during more productive periods. If bioturbation and burial were lessened, there could be a shift toward greater microbial remineralization of surface sediments, ultimately resulting in proportionally more carbon being released back into the water column as respired CO_2 rather than being sequestered deeper in the sediment.

The correlation between climate-mediated changes in POC flux, deep epibenthic animal behavior, and biologically mediated sediment mixing confirm that climate variation has far-reaching effects on the global carbon cycle, from surface productivity to deep-sea bioturbation. Long-term time-series measurements are critical to resolving the links between the surface and the actual fate of the POC being mixed by bioturbation in the context of changing climate.

Acknowledgments

We thank the members of the Smith Laboratory at the Monterey Bay Aquarium Research Institute for laboratory and editorial assistance. The animal and sediment core collections were carried out through the efforts of the skilled crews of the RVs *New Horizon*, *Atlantis*, *Thomas G. Thompson*, and *Western Flyer*, and the pilots of the submersible *Alvin* (Woods Hole Oceanographic Institution) and the ROVs *JASON II* (Woods Hole Oceanographic Institution) and *Tiburon* (Monterey Bay Aquarium Research Institute).

This research was supported by National Science Foundation grants OCE89-22620, OCE92-17334, OCE98-07103, and OCE02-4247.

References

Aller, R. C. 1982. The effects of macrobenthos on chemical properties of marine sediment and overlying water, p. 53–102. *In* P. L. McCall and M. J. S. Tevesz [eds.], Animal–sediment relations—the biogenic alteration of sediments. Topics in geobiology, v. 2. Plenum Press.

Bakun, A. 1973. Coastal upwelling indices, west coast of North America, 1946–71. NOAA Tech. Rep. NMFS SSRF-671.

Baldwin, R. J., R. C. Glatts, and K. L. Smith, Jr. 1998. Particulate matter fluxes into the benthic boundary layer at a long time-series station in the abyssal NE Pacific: Composition and fluxes. Deep-Sea Res. II **45:** 643–665.

Behl, R. J., and J. P. Kennett. 1996. Brief interstadial events in the Santa Barbara basin, NE Pacific, during the past 60 kyr. Nature **379:** 243–246.

Billett, D. S. M., B. J. Bett, A. L. Rice, M. H. Thurston, J. Galeron, M. Sibuet, and G. A. Wolff. 2001. Long-term change in the megabenthos of the Porcupine Abyssal Plain (NE Atlantic). Prog. Oceanogr. **50:** 325–348.

Bopp, L., O. Aumont, P. Cadule, S. Alvain, and M. Gehlen. 2005. Response of diatoms distribution to global warming and potential implications: A global model study. Geophys. Res. Letters **32:** L19606, doi: 10.1029/2005GL023653.

Buesseler, K. O., and others. 2007. Revisiting carbon flux through the ocean's twilight zone. Science **316:** 567–570.

Danovaro, R., and others. 2008. Exponential decline of deep-sea ecosystem functioning linked to benthic biodiversity loss. Curr. Biol. **18:** 1–8.

Guinasso, N. L., and D. R. Schink. 1975. Quantitative estimates of biological mixing rates in abyssal sediments. J. Geophys. Res. **80:** 3032–3043.

Hulthe, G., S. Hulth, and P. O. J. Hall. 1998. Effect of oxygen on degradation rate of refractory and labile organic matter in continental margin sediments. Geochem. Cosmochim. Acta **62:** 1319–1328.

Kahru, M., and B. G. Mitchell. 2002. Influence of the El Niño–La Niña cycle on satellite-derived primary production in the California Current. Geophys. Res. Lett. **29:** 1846, doi: 10.1029/2002GL014963.

Laake, J. L., S. T. Buckland, D. R. Anderson, and K. P. Burnham. 1994. Distance users guide version 2.1. Colorado State University.

Lee, C., and others. 1998. Particulate organic carbon fluxes: Compilation of results from the 1995 US JGOFS Arabian Sea Process Study. Deep-Sea Res. II **45:** 2489–2501.

Levin, L. A., N. E. Blair, C. M. Martin, D. J. DeMaster, G. Plaia, and C. J. Thomas. 1999. Macrofaunal processing of phytodetritus at two sites on the Carolina margin: *In situ* experiments using ^{13}C-labeled diatoms. Mar. Ecol. Prog. Ser. **182:** 37–54.

Levinton, J., and B. Kelaher. 2004. Opposing organizing forces of deposit-feeding marine communities. J. Exp. Mar. Biol. Ecol. **300:** 65–82.

Lohrer, A. M., S. F. Thrush, L. Hunt, N. Hancock, and C. Lundquist. 2005. Rapid reworking of subtidal sediments by burrowing spatangoid urchins. J. Exp. Mar. Biol. Ecol. **321:** 155–169.

Martin, J. H., G. A. Knauer, D. M. Karl, and W. W. Broenkow. 1987. VERTEX: Carbon cycling in the northeast Pacific. Deep-Sea Res. **34:** 267–285.

Reimers, C. E., R. A. Jahnke, and D. C. McCorkle. 1992. Carbon fluxes and burial rates over the continental slope and rise off central California with implications for the global carbon cycle. Glob. Biogeochem. Cyc. **6:** 199–224.

Ruhl, H. A. 2007. Abundance and size distribution dynamics of abyssal epibenthic megafauna in the northeast Pacific. Ecology **88:** 1250–1262.

———. 2008. Community change in the variable resource habitat of the abyssal northeast Pacific. Ecology **89:** 991–1000.

———, and K. L. Smith, Jr. 2004. Shifts in deep-sea community structure linked to climate and food supply. Science **305:** 513–515.

Schwing, F. B., T. Murphree, and P. M. Green. 2002. The Northern Oscillation Index (NOI): A new climate index for the northeast Pacific. Prog. Oceanogr. **53:** 115–139.

Smallwood, B. J., G. A. Wolff, B. J. Bett, C. R. Smith, D. Hoover, J. D. Gage, and A. Patience. 1999. Megafauna can control the quality of organic matter in marine sediments. Naturwissenschaften **86:** 320–324.

Smith, C. R., and others. 1997. Latitudinal variations in benthic processes in the abyssal equatorial Pacific: Control by biogenic particle flux. Deep-Sea Res. II **44:** 2295–2317.

Smith, K. L., R. S. Kaufmann, and R. J. Baldwin. 1994. Coupling of near-bottom pelagic and benthic processes at abyssal depths in the eastern North Pacific Ocean. Limnol. Oceanogr. **39:** 1101–1118.

Smith, K. L., Jr., R. J. Baldwin, H. A. Ruhl, M. Kahru, B. G. Mitchell, and R. S. Kaufmann. 2006. Climate effect on food supply to depths greater than 4,000 meters in the northeast Pacific. Limnol. Oceanogr. **51:** 166–176.

———, R. S. Kaufmann, and W. W. Wakefield. 1993. Mobile megafaunal activity monitored with a time-lapse camera in the abyssal North Pacific. Deep-Sea Res. I **40:** 2307–2324.

Solan, M., B. J. Cardinale, A. L. Downing, K. A. M. Engelhardt, J. L. Ruesink, and D. S. Srivastava. 2004. Extinction and ecosystem function in the marine benthos. Science **306:** 1177–1180.

Stemmann, L., G. A. Jackson, and D. Ianson. 2004. A vertical model of particle size distributions and fluxes in the midwater column that includes biological and physical processes—part I: Model formulation. Deep-Sea Res. I **51:** 865–884.

Thistle, D., J. E. Eckman, and G. L. J. Paterson. 2008. Large, motile epifauna interact strongly with harpacticoid copepods and polychaetes at a bathyal site. Deep-Sea Res. I **55:** 324–331.

Trenberth, K. E., and D. J. Shea. 1987. On the evolution of the Southern Oscillation. Mon. Weather Rev. **115:** 3078–3096.

Wakefield, W. W., and A. Genin. 1987. The use of a Canadian (perspective) grid in deep-sea photography. Deep-Sea Res. **34:** 469–478.

Wolter, K., and M. S. Timlin. 1998. Measuring the strength of ENSO—how does 1997/98 rank? Weather **53:** 315–324.

Yasuhara, M., T. M. Cronin, P. B. deMenocal, H. Okahashi, and B. K. Linsley. 2008. Abrupt climate change and collapse of deep-sea ecosystems. Proc. Natl. Acad. Sci. USA **105:** 1556–1560.

Associate editor: Markus H. Huettel

Received: 09 April 2009
Accepted: 14 June 2009
Amended: 02 July 2009